

Alma Mater Studiorum Università di Bologna
Archivio istituzionale della ricerca

Olive mill wastewater valorisation through phenolic compounds adsorption in a continuous flow column

This is the final peer-reviewed author's accepted manuscript (postprint) of the following publication:

Published Version:

Frascari, D., Molina Bacca, A.E., Zama, F., Bertin, L., Fava, F., Pinelli, D. (2016). Olive mill wastewater valorisation through phenolic compounds adsorption in a continuous flow column. CHEMICAL ENGINEERING JOURNAL, 283, 293-303 [10.1016/j.cej.2015.07.048].

Availability:

This version is available at: <https://hdl.handle.net/11585/522344> since: 2016-09-14

Published:

DOI: <http://doi.org/10.1016/j.cej.2015.07.048>

Terms of use:

Some rights reserved. The terms and conditions for the reuse of this version of the manuscript are specified in the publishing policy. For all terms of use and more information see the publisher's website.

This item was downloaded from IRIS Università di Bologna (<https://cris.unibo.it/>).
When citing, please refer to the published version.

(Article begins on next page)

This is the final peer-reviewed accepted manuscript of:

Frascari, D., et al. "Olive Mill Wastewater Valorisation through Phenolic Compounds Adsorption in a Continuous Flow Column." *Chemical Engineering Journal*, vol. 283, 2016, pp. 293-303.

The final published version is available online at :
<http://dx.doi.org/10.1016/j.cej.2015.07.048>

Rights / License:

The terms and conditions for the reuse of this version of the manuscript are specified in the publishing policy. For all terms of use and more information see the publisher's website.

This item was downloaded from IRIS Università di Bologna (<https://cris.unibo.it/>)

When citing, please refer to the published version.

OLIVE MILL WASTEWATER VALORISATION THROUGH PHENOLIC COMPOUNDS ADSORPTION IN A CONTINUOUS FLOW COLUMN

Dario Frascari ^{a,*}, Aurora Esther Molina Bacca ^a, Fabiana Zama ^b, Lorenzo Bertin ^a, Fabio Fava ^a, Davide Pinelli ^a

^a *Department of Civil, Chemical, Environmental and Materials Engineering, University of Bologna, Via Terracini 28, 40131 Bologna, Italy*

^b *Department of Mathematics, University of Bologna, Piazza di Porta San Donato 5, 40126 Bologna, Italy*

* Corresponding author. Tel.: +39 051 2090416. E-mail address: dario.frascari@unibo.it (D. Frascari).

ABSTRACT

A continuous-flow adsorption/desorption process for the recovery of phenolic compounds (PCs) from olive mill wastewaters (OMWs) was developed in a 0.53 m packed column, using a previously selected resin (Amberlite XAD16) and an actual OMW. The main goals of the study were (i) to evaluate the PC adsorption/desorption performances of XAD16 by means of adsorption isotherms and adsorption/desorption breakthrough tests, and (ii) to develop a reliable model of the process. A combination of centrifugation and microfiltration resulted necessary to attain a high suspended solid removal (98.5%) and thus avoid clogging of the packed bed. The quality of two packing procedures was evaluated by means of frontal analysis tests. XAD16 performed well in terms of both adsorption yield at 20% breakthrough (87-88%) and PC/COD selectivity (PC/COD adsorption constant = 7-9). The desorption solvent (acidified ethanol) was effectively regenerated by vacuum distillation. The adsorption breakthrough curves were successfully simulated with a 1-D convection/dispersion model with mass-transfer ($R^2 = 0.95-0.99$; $k_{La} = 0.8-2.5 \cdot 10^{-3}$ 1/s), whereas an equilibrium adsorption model with dispersion failed to predict the experimental data. In the perspective of a process scale-up, the simulation of the best-performing operational condition was used to evaluate the process performances for different column lengths (0.5-10 m). A precise and automated HPLC method for total PC measurement was developed and compared to the traditional Foulon-Ciocalteu methodology. Further research is needed to optimize the desorption step, to scale up the process and to evaluate the long-term resin performances.

Keywords: adsorption, olive mill wastewater, phenolic compounds, resin, mass-transfer, modeling.

This is the author-accepted manuscript. The final version has been published by the Elsevier in Chemical Engineering Journal (Vol. 283, pp. 293-303) and is available to subscribed users at:

<https://www.sciencedirect.com/science/article/pii/S1385894715010141>

(doi: 10.1016/j.cej.2015.07.048)

1. Introduction

The beneficial health properties of olive oil are well known because of its high content in phenolic compounds (PCs). Recent studies showed the antioxidant, anti-inflammatory and antimicrobial potential of PCs [1]. Olive oil can be obtained by means of two different processes. The first one is a two-phase procedure, in which oil is separated from the solid mass of olive milling, producing olive oil and a pasty residue very difficult to handle. The second process is a three-phase system, in which water is added to enhance oil separation and recovery. In this way, oil and vegetation waters are separated from the solid phase, then olive oil is separated from olive mill wastewater (OMW) by decantation. OMW is easier to treat than the residue of the two-phase process, and it has a higher PC content [2]. PCs distribute between olive oil and OMW, but the latter contain about 95% of the PC content in the original olives, as a result of the high solubility of PCs in water [2,3].

Given the high production of olive oil ($3.3 \cdot 10^6$ t/y worldwide in the 2013/14 season; [4]) and the high OMW/olive oil ratio ($7\text{--}8 \text{ m}^3_{\text{OMW}}/\text{t}_{\text{olive oil}}$), OMW production is extremely large: $23\text{--}26 \cdot 10^6 \text{ m}^3_{\text{OMW}}/\text{y}$ are produced in Mediterranean, where 98% of the world olive oil production is concentrated [4]. OMWs represent a major environmental concern due to their high COD content (20-60 g/L), high toxicity and bad smell. The high PC content (0.1-18 g/L) inhibits seed germination and plant growth and changes the physicochemical and biological soil properties [2;5-8]. For these reasons, although OMWs have traditionally been discharged directly in the olive tree fields, most countries have recently banned this practice, thus imposing OMW treatment. Furthermore, PCs inhibit aerobic and anaerobic biological processes that can be applied to turn OMWs into irrigation waters through the removal of their COD [9].

On the other hand, PCs have highly beneficial properties, and in particular the antioxidant properties of oleuropein, tyrosol and hydroxytyrosol are of high interest. Hydroxytyrosol, the most abundant PC in OMWs, has particularly high antioxidant, antibacterial, anti-inflammatory and anti-angiogenic activities [1,2,6,10-13]. Thus, hydroxytyrosol is one of the most valuable and expensive PCs, with a high demand in the pharmaceutical, food and cosmetics fields [11].

Several methodologies for PC recovery from OMW were proposed, including solvent extraction, membrane separation, centrifugation and chromatographic procedures. Solvent extraction is the most commonly employed technique to extract PCs from OMWs: acidic ethyl acetate is the most effective solvent, but supercritical fluids and acidified ethanol were successfully used [2,11,14-16]. Interesting results were obtained by enhancing solvent extraction with ultrasounds [17]. Different combinations of membrane separation processes, such as ultrafiltration, microfiltration, reverse osmosis and membrane distillation have been proposed either as a pretreatment step before further unit operations, or as a complete PC removal process [18-21]. Cloud Point Extraction (CPE) was also investigated for PC recovery from OMW, using surfactants such as Genapol X-080, Triton X-100 and PEG-8000 [22,23]. Other emerging technologies are today investigated (i.e radio-frequency drying, electro-osmotic dewatering, ultrasound-assisted extraction, high voltage electrical discharge, pulsed electric field) at research level and in some cases applied in the food industry [24]. Many technologies can be used to recover a variety of valuable compounds from food by-products [25].

Adsorption represents an interesting solution for the recovery of PCs from OMW. This technology allows to separate selected compounds from dilute solutions with a relative simplicity of design, operation and scale up, a high capacity and a favorable rate. It is also characterized by ease of regeneration and low costs [26]. The main drawback is the lack of selectivity, that can lead to a product that sometimes requires further purification. Several studies conducted in small-scale batch conditions focused on the comparison of the PC sorption isotherms and efficiencies of different resins [6,27-34]. However, a limited number of studies focused on the development of continuous-flow processes for the adsorption/desorption of PC mixtures [35-41]. Of these studies, only one was performed with actual OMW [35], while the others were aimed at the recovery of PCs from other natural sources or from synthetic mixtures. Furthermore, the modeling of the continuous-flow adsorption/desorption process was generally neglected in the above-mentioned studies. Indeed, to the best of the authors' knowledge, the only study that focused on the modeling of PC dynamic adsorption/desorption was not referred to OMW PCs [38], whereas a few other works modeled the adsorption of phenol from a synthetic solution of phenol in water [e.g., 42-44]. Therefore, further work is needed with regard to the application of general adsorption optimization criteria to the specific case of PC separation from OMW and to the modeling of OMW PC adsorption/desorption, a crucial step towards the development of an industrial-scale process. On the other hand, an analysis of the scientific literature shows that in order to obtain a marketable PC-containing product a multiple phase separation and enrichment process is generally required [45].

The goal of this work was to perform the preliminary development and modeling of a continuous-flow process of PC separation from a real OMW via adsorption/desorption using a column packed with a non-ionic styrene-divinylbenzene resin (Amberlite XAD16). PC separation represents the first step of a wider OMW valorization process, in which dephenolized OMW feeds a polyhydroxyalkanoate production step, whose effluent is sent to anaerobic digestion [46]. The resin and the desorption solvent used in this study were selected in the framework of previous works conducted by the same research group [6,27,28]. In those works, five resins with different physical properties (Amberlite XAD4, XAD7, XAD16, IRA96 and Isolute ENV+) were compared by means of batch tests for their adsorption and desorption capacities towards (i) an aqueous solution of ten target phenolic compounds typically occurring in OMWs [27], and (ii) the PCs contained in two real OMWs [6]. The overall evaluation of the adsorption and desorption performances led to the selection of Amberlite XAD16 as the adsorbent, and of ethanol acidified with HCl 0.5 ml/100 mL as the desorbing agent. Furthermore, Scoma et al. [28] showed that the process was characterized by nearly constant performances during 10 consecutive batch adsorption and desorption cycles performed with the same resin and with the same ethanol, regenerated by distillation. The present work had the following specific goals: (i) to evaluate the PC adsorption/desorption performances attainable by means of a continuous-flow process performed in a 0.525 m column at two superficial velocities; and (ii) to perform a preliminary modeling and optimization of the adsorption process. As a secondary outcome, this work led to a comparison between the Foulin-Ciocalteu analytical method, typically utilized in the literature to determine total PCs, and an alternative, less time-consuming HPLC method. The main novel element of this study lies in the development, modeling and preliminary optimization of a continuous flow adsorption/desorption process aimed at OMW PC separation.

2. Materials and Methods

2.1 OMW, resin and chemicals

The OMW used in this study, labeled “Imperia 2012”, was provided by an olive mill located near Imperia, in the North-West of Italy. The main characteristics of the tested OMW are reported in Table 1.

The adsorption solid phase is the non-ionic styrene-divinylbenzene resin Amberlite XAD 16 (DOW Chemicals Europe GmbH, Horgen, Switzerland). Its main characteristics are described in the Table 2. The resin was activated as follows: i) resin soaking with acidified ethanol (0.5% HCl 0.1N), ii) overnight drying at 105°C, iii) second resin soaking with acidified ethanol, iv) washing with demineralized water (twice) [28]. Finally, the activation solvent was removed by siring aspiration and a mass of activated and hydrated resin (28.3% w/w resin, 71.7% w/w water) was obtained.

The desorption-regeneration solvent, the HPLC mobile phase components, gallic acid, the Folin-Ciocalteu reagent, sodium carbonate, sodium chlorate, sulfuric acid and the solvents for resin activation were obtained from Sigma Aldrich (Milan, Italy). The COD Test Tubes were acquired from Aqualytic (Dortmund, Germany).

2.2 Analytical methods

Total Phenols. Two different approaches were applied and compared to measure total PCs: the conventional colorimetric test developed by Folin and Ciocalteu [47] and an in-house developed HPLC method. In the Folin-Ciocalteu (FC) method, 25 mL flasks, carefully cleaned with sulfuric acid 25% and washed with de-ionized (DI) water, were filled with 12.5 mL of DI water, 125 μ L of sample (diluted as required, to avoid absorbance signal saturation) and 1.25 mL of FC reagent. After 2 minutes, the reaction was quenched by adding 3.75 mL of sodium carbonate (20% w/v). Finally, the flasks were diluted to the volume mark, and left at 75°C for two hours. Then, the absorbance was read at 765 nm with a Cary 100Scan UV spectrophotometer (Agilent, Santa Clara, California), using as reference a dephenolized OMW obtained by repeated adsorptions with the Amberlite XAD16 resin until the attainment of a final PC content < 1% of the original PC level in the OMW, and then treated with FC reactants. The method was calibrated with acid gallic as external standard.

For the HPLC method, a Jasco 880 pump, a Jasco 875-UV Intelligent UV/vis detector (Easton, Maryland) set at 264 nm and a C18 Kinetex 2.6 μ m 100A Phenomenex column were utilized. The flow was set at 1.0 mL/min. The following mobile phase gradient was applied: 0-4 minutes, 100% phase A (HPLC water with 0.1% orthophosphoric acid); 4-6 minutes, 70% phase A and 30% phase B (acetonitrile); 6-15 minutes 70% phase A and 30% phase B. The mobile phase gradient was designed to merge all the phenolic peaks into a single broad peak. This approach makes the analysis faster and the method more sensitive, but it prevents the identification of the single compounds. An internal standard (gallic acid 50 mg/L) was added in each HPLC analysis.

Total Solids. 20 mL of OMW were dried overnight at 105°C in a porcelain crucible, cooled in a desiccator and weighted using a 4-digit analytical balance. The procedure was applied in triplicate. *Suspended Solids.* 20 mL of OMW were filtered with a 0.45 μ m ALBET cellulose nitrate

membrane filter and placed in a Whatman vacuum filtration system. The filter was dried at 105°C for two hours, cooled in a desiccator and weighted. The procedure was applied in triplicate. *Dissolved solids* were calculated as the difference between total and suspended solids.

COD was measured spectrophotometrically using the Aqualytic COD Vario Tubes (range: 0-1500 mg_{O2}/L). Each tube contained potassium permanganate in an acid medium, to which 2 mL of diluted sample were added. The tubes were then left at 150°C for 2 hours in a ECO16 Velp Scientifica thermoreactor (Monza, Italy). After cooling the tubes for 30 minutes, the absorbance of each sample was measured at 610 nm.

Total carbohydrates were determined by a modified Dubois method [48]. The calibration curve was made with glucose as standard. All measurements were done in duplicate. *Total lipids* were evaluated as reported in [49] using as a standard the olive oil produced at the industrial plant to which the tested OMW belongs. *Total proteins* were determined with the Bradford method [50], by using the commercial protein assay dye reagent concentrate from BioRad (Milano, Italy).

Density and pH. A 100 mL ITI Tooling pycnometer was used for OMW density estimation, whereas pH was measured with an EUTECH Instruments pH 2700 Series pH-meter (Thermoscientific, Waltham, Massachusetts).

2.3 Adsorption isotherms

The adsorption isotherms of the total PCs contained in the tested OMW were studied both at 21 and 30°C, the two operational temperatures of the PC adsorption experiments described in Section 2.7. Different amounts (0.1, 0.2, 0.5, 1.0 or 2.0 g) of dry resin were introduced into 50 mL glass vials. Two vials were set up for each amount of resin. The resin activation procedure (Section 2.1) was performed inside each vial. After adding 20 mL of OMW, the vials were placed in a rotatory shaker (140 rpm, 21 or 30°C) for 2 h. Preliminary adsorption tests characterized by OMW samplings every 15 minutes showed that liquid-solid equilibrium was attained after about 1 hour. The equilibrium PC concentration in the liquid phase was evaluated with the HPLC method. The equilibrium concentration in the solid phase $C_{S,PC,eq}$ was then calculated as:

$$C_{S,PC,eq} = (C_{L,PC,0} \cdot V_{L,added} - C_{L,PC,eq} \cdot V_{L,final}) / m_S \quad (1)$$

where m_S is the dry resin mass, $C_{L,PC,0}$ and $C_{L,PC,eq}$ are the initial and final PC concentrations in the liquid, whereas $V_{L,added}$ and $V_{L,final}$ are respectively the OMW volume added to the solid and the final liquid volume resulting from the sum of the added OMW and the water initially contained in the activated resin. The 95% confidence intervals associated to $C_{S,PC,eq}$ were calculated using standard error propagation rules, on the basis of the 95% confidence intervals associated to the experimental measurements of $C_{L,PC}$, V_L and m_S . The 95% confidence interval associated to $C_{L,PC}$ was estimated from 15 replicated HPLC analyses of a reference gallic acid standard solution (50 mg/L).

2.4 OMW pre-treatment

To avoid a gradual pressure drop increase in the adsorption column and eventually the complete clogging of the inlet section, a suitable OMW pre-treatment aimed at suspended solids removal must be performed. For this reason, an OMW 3-step pre-treatment was set up. The first step consisted in centrifugation at 4000 rpm for 30 minutes, using a ThermoScientific SC16R centrifuge (Waltham, Massachusetts). The second and third step consisted in a continuous in-line microfiltration performed respectively with 25 µm and 11 µm GE Healthcare Life Science Whatman filters, placed in plastic filter holders. Filtration was performed at a 1 m/h superficial velocity.

2.5 Fluid dynamic tests

To evaluate the packing quality and the fluid dynamic behavior of the packed bed, a frontal analysis experimental test was carried out after each packing procedure. A 0.04 M NaCl solution was fed from the top of the column at a superficial velocity of 1.22 m/h. At the column outlet, the electrical conductivity (EC) was measured with an EUTECH Instruments 2700 series conductimeter.

The packing quality was evaluated by means of two approaches based on the analysis of the retention times distribution curve (RTD) obtained by calculating point by point the derivative of the sigmoidal experimental curve of normalized EC versus time provided by the fluid-dynamic test [51]. The first approach is based on the *Theoretical Plate Model*: the number of theoretical plates N_{tp} can be evaluated as:

$$N_{tp} = 5.54 \cdot (t_R/w_{1/2})^2 \quad (2)$$

where t_R indicates the retention time of the RTD curve and $w_{1/2}$ its width at half-height. The height equivalent to a theoretical plate (*HETP*) can then be calculated as L/N_{tp} , where L indicates the column length. A high-quality column packing is characterized by a value of $HETP/d_p < 3$, where d_p indicates the average size of the packing particles [52]. The second approach is based on the *asymmetry factor* (A_s), defined as the ratio between the leading and tailing semi-width of the peak at 10% of the peak height, and representing the peak deviation from a Gaussian curve. Its value should be as close as possible to 1 [52].

The frontal analysis data were also utilized to estimate the effective porosity (ε) and longitudinal dispersivity (α_L) of the resin packed bed. The former parameter was evaluated directly from the RTD curve according to the procedure proposed by Levenspiel [51], whereas the latter was estimated by best-fit of the experimental outlet concentrations with a 1-D convection-dispersion model:

$$\delta_i \cdot \frac{\partial C_{L,i}}{\partial t} = -v_{int} \cdot \frac{\partial C_{L,i}}{\partial z} + D_{eq} \cdot \frac{\partial^2 C_{L,i}}{\partial z^2} \quad (3)$$

In Eq. (3) the retardation factor δ_i , equal to $1 + K_{eq,i} \rho_b / \varepsilon$, was set to 1 due to the absence of NaCl adsorption, the interstitial velocity v_{int} was calculated as $Q / (S_t \cdot \varepsilon_{resin})$ for the resin bed ($10 \text{ mm} < z < 515 \text{ mm}$) or $Q / (S_t \cdot \varepsilon_{sand})$ for the two sand layers ($z < 10 \text{ mm}$ and $515 \text{ mm} < z < 525 \text{ mm}$), and the equivalent diffusion coefficient D_{eq} was approximately expressed as $\alpha_{L,resin} \cdot v_{int,resin}$ or $\alpha_{L,sand} \cdot$

$v_{int,sand}$ [53]. The integration of Eq. (3) was performed with the time-dependent convection/diffusion module of the finite element PDE solver Comsol Multiphysics 3.5a, using as input values the estimates of ε_{sand} and $\alpha_{L,sand}$ obtained in preliminary tests and the value of ε_{resin} estimated as described above. As for $\alpha_{L,resin}$, its best-fit value and the 95% confidence interval were determined by applying the Gauss-Newton method, following the procedure illustrated by Englezos and Kalogerakis [54] and later adapted to convection-dispersion problems by Zama et al. [55]. In particular, the integration of Eq. (3) was repeated for different values of α_L , until the minimization of the sum of the squared residuals between experimental and calculated values at the column outlet. As a convergence criterion, the Gauss-Newton algorithm was stopped when the relative variation in $\alpha_{L,resin}$ resulted $< 10^{-3}$. This procedure was implemented by means of a dedicated MATLAB code.

2.6 Adsorption column packing

The semicontinuous adsorption / desorption tests were performed in a glass column (length 0.525 m, inner diameter 0.020 m). After placing a 10-mm layer of quartz sand at the bottom of the column, the latter was filled with activated XAD16 resin using the Dynamic Axial Compression (DAC) technique, by applying two alternative procedures. The first procedure was based on the use of a slurry prepared by mixing equal volumes of activated resin and of a 10% solution of acidified ethanol (HCl 0.1 N 0.5%) in water [56]. The slurry resin was then divided into 4 aliquots. After pouring each aliquot, the column was filled with acidified ethanol and the solvent was extracted and recirculated downwards with a Masterflex L/S 0.1HP 1-100 RPM pump (Cole-Parmer, Vernon Hill, Illinois) until the stable settling of the resin. Then, a further aliquot was fed and the procedure was repeated. The second procedure was based on the use of two activated resin slurries, prepared with DI water (100 g_{dry_resin}/L_{DI water} and 600 g_{dry_resin}/L_{DI water}, respectively). Each slurry was sonicated for 5 minutes in order to remove the air trapped in the resin beads. Initially, 150 mL of the first slurry were poured on the sand layer and left to natural settling for one hour. Then, after recirculating DI water downwards until the stable settling of the resin, 25 mL of the second slurry were added in three steps, and a further DI water recirculation was applied. As a final step in both column packing procedures, a further 10-mm quartz sand layer was placed at the top of the resin and the column was flushed downwards overnight with DI water.

The packing procedure with demineralized water performed markedly better than that employing acidified ethanol, with: i) a slight increase in the number of theoretical plates (from 93 to 117), a 23-fold reduction in terms of $HETP/d_p$ (from 0.32 to 7.5) and an asymmetry factor significantly closer to 1 (0.82 for the acidified ethanol procedure, 1.1 for the demineralized procedure). The demineralized water procedure was thus utilized for the PC adsorption/desorption tests object of this work.

2.7 Adsorption process: breakthrough tests and simulations

After packing the column with the second procedure, two adsorption breakthrough tests were performed with the experimental OMW, at a superficial velocity of 0.48 m/h (bt 1) or 1.44 m/h (bt 2). These velocities were selected on the basis of the values typically used in similar studies [35-41]. Due to a change in room temperature between the first and the second test, bt 1 was operated at 21°C, and bt 2 at 30°C. The pre-treated OMW was fed downwards with a Masterflex L/S 0.1 HP 1-100 RPM peristaltic pump. Both pressure drop and temperature were measured hourly. The total PC concentration was measured with the HPLC method in OMW samples taken every hour from the column exit and every 3 hours from the inlet, whereas COD was measured in selected samples at the column inlet and outlet. The average PC concentration and COD values at the inlet were used to normalize the corresponding outlet values. Continuous-flow dephenolization processes are typically stopped in correspondence with the attainment of a relatively low PCs level at the column outlet, the break-point (e.g., $C_{OUT}/C_{IN} = 0.10-0.20$). However, the experimental tests were continued up to outlet normalized PC concentrations varying between 0.56 (bt 1) and 0.65 (bt 2), in order to increase the extension of the experimental breakthrough curve, and thus the reliability of the subsequent model simulations. The above-reported normalized concentrations correspond for both tests to a total feeding time equal to 25 hydraulic residence times (HRT , calculated as $V_{resin} \cdot \varepsilon_{resin} / Q + V_{sand} \cdot \varepsilon_{sand} / Q$).

The experimental normalized PC and COD breakthrough curves were interpreted by means of two types of 1-D convection-dispersion models, in order to study the key controlling phenomena, to evaluate the process efficiency and to set up the basis for a model-based optimization and scale-up of the process. A first set of simulations was performed under the hypothesis of local adsorption equilibrium and linear adsorption isotherm (on the basis of the results of the PC isotherm studies). In these simulations, the normalized PC and COD concentrations were interpreted with Eq. (3), with the retardation factors δ_{PC} or δ_{COD} expressed as $(1 + K_{eq,PC} \cdot \rho_b / \varepsilon_{resin})$ or $(1 + K_{eq,COD} \cdot \rho_b / \varepsilon_{resin})$ for the resin layer ($10 \text{ mm} < z < 515 \text{ mm}$) and set to 1 for the two sand layers. The bulk density ρ_b was calculated as the mass of dry resin introduced during the packing process divided by the volume of the column portion occupied by resin. Using the estimates of ε_{resin} and $\alpha_{L,resin}$ obtained from the fluid-dynamic test as input values, the equilibrium constants $K_{eq,PC}$ and $K_{eq,COD}$ relative to each breakthrough test were estimated by best-fit on the corresponding experimental concentrations following the Gauss-Newton method described in Section 2.6. As a convergence criterion, the algorithm was stopped when the average parameter variation resulted $< 10^{-3}$.

In a second set of simulations, conducted under the hypothesis of not negligible mass-transfer resistance and linear isotherm, the normalized outlet PC and COD were interpreted with the following equation:

$$\frac{\partial C_{L,i}}{\partial t} = -v_{int} \cdot \frac{\partial C_{L,i}}{\partial z} + D_{eq} \cdot \frac{\partial^2 C_{L,i}}{\partial z^2} - k_L a \cdot \left(C_{L,i} - \frac{C_{S,i}}{K_{eq,i}} \right) \quad (4)$$

where $C_{L,i}$ indicates the PC or COD liquid phase concentration, $C_{S,i}$ the corresponding solid-phase concentration (g/g_{dry resin}) and $k_L a$ the mass-transfer coefficient. In this model internal and external mass transfer phenomena are expressed by means of an overall volumetric coefficient and an overall driving force [57]. The same $k_L a$ value was assumed to be valid for PCs and COD. The presence of a solid-phase concentration independent of the liquid-phase concentration requires the addition of the mass-balance relative to $C_{S,i}$, characterized by the absence of any convection or dispersion:

$$\frac{\rho_b}{\epsilon} \cdot \frac{\partial C_{S,i}}{\partial t} = k_L a \cdot \left(C_{L,i} - \frac{C_{S,i}}{K_{eq,i}} \right) \quad (5)$$

In these simulations, while $k_L a_{sand}$ and $K_{eq,sand}$ (for $z < 10$ mm and 515 mm $< z < 525$ mm) were set equal to zero, both $K_{eq,PC}$ and $k_L a_{resin}$ (for 10 mm $< z < 515$ mm) were estimated by best-fit on the experimental PC concentrations following the Gauss-Newton method, and the resulting value of $K_{eq,PC}$ was compared to that obtained from the corresponding PC isotherm. In the COD simulations, only $K_{eq,COD}$ was estimated by best-fit on the experimental COD concentrations, whereas the $k_L a_{resin}$ best estimate obtained from the corresponding PC breakthrough test was used as an input value. For both sets of simulations, the quality of each best fit was evaluated by means of the correlation coefficient R^2 , defined so as to allow the comparison of models with different numbers of parameters [58]:

$$R^2 = 1 - \left(\frac{\sum_{j=1}^N (C_{L,measured,j} - C_{L,calculated,j})^2}{N - P - 1} \right) / \left(\frac{\sum_{j=1}^N (C_{L,measured,j} - \bar{C}_{L,measured})^2}{N - 1} \right) \quad (6)$$

where N indicates the number of experimental data and P the number of parameters evaluated by best fit on the experimental data (1 or 2, depending on the set of simulations).

For each breakthrough test, the best-fitting simulation was utilized to estimate two types of parameters useful for the evaluation of the adsorption process performance: the PC and COD adsorption yields $Y_{ads,PC}$ and $Y_{ads,COD}$, and the resin utilization efficiency (or percent utilization) η_{resin} , complementary to the normalized length of unused bed [57]. Both types of parameters were evaluated relatively to the fraction of breakthrough curve comprised between $C_{PC,OUT}/C_{PC,IN} = 0$ and $C_{PC,OUT}/C_{PC,IN} = 0.20$, so as to obtain data representative of a hypothetical industrial process. The adsorption yields $Y_{ads,i}$ were evaluated as $m_{i,sorbed,20\%} / m_{i,fed,20\%}$, where $m_{i,sorbed,20\%}$ indicates the PC or COD mass adsorbed until the attainment of a 20% outlet normalized PC concentration, and $m_{i,fed,20\%}$ indicates the corresponding PC or COD mass fed to the column. $m_{i,sorbed,20\%}$ was estimated as:

$$m_{i,sorbed,20\%} = m_{i,fed,20\%} - m_{i,out,20\%} \quad (7)$$

where $m_{i,out,20\%}$ is the mass lost in the outlet up to the 20% breakpoint. Eq. (7) neglects the liquid phase PC content at the 20% breakthrough point, which is generally negligible and whose fate is determined by the process choices on how to move from the adsorption phase to the regeneration step. $m_{i,out,20\%}$ was calculated by integrating the breakthrough curve:

$$m_{i,out,20\%} = Q \cdot \int_0^{t_{20\%}} C_{L,i,OUT} \cdot dt \quad (8)$$

A more compact expression for $m_{i,sorbed,20\%}$ can be obtained combining Eqs. (7) and (8):

$$m_{i,sorbed,20\%} = Q \cdot \int_0^{t_{20\%}} (C_{L,i,IN} - C_{L,i,OUT}) \cdot dt \quad (9)$$

The integrals in Eqs. (8) and (9) were calculated by numerical integration of the best-fitting simulated outlet concentrations.

The resin utilization efficiency η_{resin} represents the fraction of adsorption bed capacity actually utilized. It was evaluated, only for PC adsorption, as:

$$\eta_{resin} = m_{PC,sorbed,20\%} / m_{PC,sorbed,sat} \quad (10)$$

where $m_{PC,sorbed,sat}$ indicates the PC mass theoretically adsorbed by the resin upon saturation of the sorption capacity. If the equilibrium constant is known, $m_{Ph,sorbed,sat}$ can be evaluated as $K_{eq,PC} \cdot C_{L,PC,IN} \cdot m_{resin}$. Alternatively, by extrapolating the best fitting simulation, it can be estimated as $Q \cdot \int_0^{t_{99.9\%}} (C_{L,i,IN} - C_{L,i,OUT}) \cdot dt$ where $t_{99.9\%}$ indicates the time theoretically corresponding to the attainment of an outlet PC concentration equal to 99.9% of the inlet value.

2.8 Desorption-regeneration tests

To desorb and recover the PCs, at the end of each adsorption test acidified ethanol (0.5% v/v HCl 0.1N) was fed from the bottom of the column with a Masterflex L/S 0.1 HP -1-100 RPM pump. The solvent flow rate was initially set to the OMW flow rate of the corresponding adsorption test. However, due to the increase in solvent viscosity associated to the increase in PC dissolved concentration, a gradual decrease in solvent flow rate was required in order to maintain the total pressure at the column inlet < 2 bars. Desorption was continued until the attainment of a PC concentration $< 5\%$ of the average inlet concentration during the adsorption step. This criterion corresponded to a total desorption time equal to 5 *HRTs*. The desorbed extract was submitted to low-pressure distillation in a rotatory evaporator (LABOROTA 4002 Heidolph, Schwabach, Germany), in order to regenerate the solvent and recover the desorbed matter. Temperature was kept at 30°C with a Heizbad WB Heidolph thermostated bath (Schwabach, Germany), and vacuum (0.5 bar of absolute pressure) was applied with a Vacuubrand diaphragm vacuum pump (Wertheim, Germany). Water at 5°C was used as coolant. Preliminary tests indicated that desorption with acidified ethanol is also an effective resin regeneration method. On the basis of the integral PC concentration measured in the ethanol collected from the column outlet, the desorption yield $Y_{des,PC}$ was evaluated as $m_{PC,desorbed,total} / m_{PC,sorbed,total}$.

3 Results and Discussion

3.1 Ancillary results: PC analytical method selection and OMW pre-treatment

The HPLC PC method was studied in order to develop a fast, precise and automatable analytical tool to assess the adsorption performances, whereas it was not meant as a substitute of the Foulon-Ciocalteu (FC) method, widely adopted for PC content assessment. Indeed, neither method guarantees that all and only phenolic compounds will be detected: the HPLC method could in principle sum non-phenolic compounds to the actual PCs and/or fail to detect specific PCs, whereas the FC method can be characterized by an interference due to other organic compounds present in OMW (i.e. proteins and carbohydrates). Both the traditional FC method and the proposed HPLC method treat the PC mixture as a pseudo component, expressing the total PC concentration as specific PC equivalent (gallic acid in the present work). These methods thus avoid the

complexity of taking into account the contribution of each single compound. This approximation is less severe in the case of the FC method, which recognizes the chemical functionality by the selective colorimetric reaction. For that reason, some preliminary cross-checks between the two methods were carried out.

In the first place, the PC content in the studied Imperia 2012 OMW was measured using both methods (Table 3, 2nd column). As expected, the total PC concentrations measured with the two methods were not equal, and a 36% lower value was observed with the HPLC method. In order to strengthen the comparison between the two methods, the same type of analysis was applied to a different OMW, characterized by a higher PC concentration and by a different PC composition (Gallipoli 2012 OMW, produced in the Apulia Region in Southern Italy). As shown in the 3rd column of Table 3, the agreement between the two methods is similar. On the other hand, the low relative errors associated to the HPLC method (equal to about 1/3 of the FC relative errors) indicate that the HPLC method is significantly more precise.

Finally, PC concentration in the samples taken at the column outlet during one of the breakthrough tests performed in this work (bt 2, conducted at 30°C and 1.44 m/h) was analyzed with both methods. This validation test was aimed at checking the capacity of the HPLC method to mimic the FC results in the characterization of the adsorption process. As different PCs are eluted at different breakthrough times, the outlet composition is continuously changing. Thus, this test is far more severe than the simple comparison of total OMW PCs. The results are shown in Fig. 1 in terms of dimensionless outlet PC concentration versus dimensionless time, defined as time / HRT . The deviation between the two methods ranged between 0.4% and 17%, with an average value (10%) comparable to the relative analytical errors. The scrutiny of Fig. 1 confirms the higher precision of the HPLC method. On the basis of these results, the HPLC method was selected as the reference method for this study.

With regards to the OMW pre-treatment required before feeding the adsorption column, the suspended solid removal was equal to 91.5% after the initial centrifugation step (4000 rpm, 30 minutes), and to 98.5% after the entire pre-treatment sequence (centrifugation + 25 μ m filtration + 11 μ m filtration). Despite the high removal obtained with only centrifugation, preliminary breakthrough tests performed with centrifuged but unfiltered OMW led to a marked increase in pressure drop across the column (from 0.1 to 1 bar). Conversely, the complete pre-treatment allowed the operation of 36-hour breakthrough tests with modest pressure drop increases (from 0.1 to 0.3 bar, corresponding to a total pressure in the column inlet of 1.1-1.3 bars), that were completely reversed during the subsequent desorption step. The PC removal associated to the complete pretreatment sequence, measured with the HPLC method, resulted equal to 7-8%

3.2 Fluid dynamic characterization

The column was emptied and re-packed with fresh XAD16 resin after the first adsorption/desorption test and a fluid-dynamic test with NaCl as tracer was performed after each column packing, in order to evaluate the repeatability of two consecutive packings in terms of bulk density, resin porosity and resin longitudinal dispersivity. As a representative case, the experimental dimensionless NaCl concentration at the column exit and the corresponding best-fitting simulation performed with Eq. (3) with retardation factor $\delta = 1$ are shown in Fig. 3 for the fluid-dynamic test performed before test bt 1. As shown in Table 4, the packing procedure with DI water was characterized by a high repeatability in terms of bulk density, resin porosity and resin longitudinal dispersivity, with variations in the 2-4% range. The Gauss-Newton algorithm for the evaluation of $\alpha_{L,resin}$ converged after 10 iterations. As shown in Fig. 3, the 1-D fluid-dynamic model

utilized to estimate $\alpha_{L,resin}$ and ε_{resin} (Eq. (3)) allowed the attainment of a very good fit of the experimental tracer concentrations ($R^2 = 0.9994$), and was thus considered a suitable basis for the interpretation of the PC and COD concentrations with the 1-D transport model with adsorption described in Section 2.7.

3.3 Polyphenol adsorption isotherms

The solid- and liquid-phase PC concentrations relative to the isotherms performed at 21°C and 30°C are shown in Fig. 2. The high 95% confidence intervals that characterize the right-hand part of the isotherm are due to the fact that the higher solid-phase concentrations, calculated with Eq. (1), result from the subtraction of aqueous-phase concentrations very close to each other. Despite the quite high data dispersion, the points seem to follow a slightly pronounced sigmoidal curve that might result from the competitive adsorption of multiple PCs, measured by the selected analytical method as a single equivalent compound. Nevertheless, as shown in Fig. 2, at both temperatures a linear interpolation – corresponding to the initial linear part of the Langmuir curve – resulted in acceptable R^2 values (0.93). Indeed, the almost linear behavior of these isotherms is reasonable considering that the resin adsorption capacity (370 mg/g_{dry resin}, referred to medium molecular weight compounds; Table 2) is almost 10 times higher than the maximum concentration of sorbed PCs attained in these tests (40 mg/g_{dry resin}). Thus, other types of interpolations were not taken into consideration. The best estimates of $K_{eq,PC}$ obtained from the isotherms of Fig. 2 (Table 4, last line) are in agreement with the results of Bertin et al. [96], who tested XAD16 on a different OMW. Although Bertin et al. [6] used both a Langmuir and a Freundlich isotherm, their experimental data correlate very well with a straight line corresponding to an equilibrium constant of 58 L/kg_{dry resin}, versus 42-73 L/kg_{dry resin} in this study. Agalias et al. [35], who tested XAD 16 on a Greek OMW, performed isotherm tests only on a hydroxytyrosol synthetic solution. They applied a Freundlich isotherm that at 20°C predicts a solid concentration in equilibrium with the maximum liquid concentration tested in our isotherms (0.6 g/L) of 1 mmol/g of hydroxytyrosol, versus 0.24 mmol/g of gallic acid equivalent in our 21 °C isotherm. Other authors mostly worked with PCs from other sources (apple juice [36], blueberries [37], rice straw [40]) or with single phenols [38, 59], and tested different types of sorbents. They generally reported equilibrium data better described by Langmuir or Freundlich isotherms, but their data can not be compared with those of this study.

3.4 Phenolic compounds and COD breakthrough tests

The normalized PC and COD concentrations obtained at the column outlet during breakthrough tests bt 1 (21°C, $v_{sup} = 0.48$ m/h) and bt 2 (30°C, $v_{sup} = 1.44$ m/h) are plotted in Figs. 4a and 4b versus dimensionless time, whereas the main process performances are reported in Table 4. Fig. 4 shows that the total COD elutes significantly faster than the PCs, indicating a high selectivity of the tested XAD16 resin towards PCs. Nevertheless, some non-phenolic compounds were adsorbed and therefore present in the product eventually recovered from the column, as shown in Fig. 4c and discussed further on in this Section.

As illustrated in Section 2.7, a first attempt to simulate the PC and COD experimental outlet concentrations was performed with Eq. (3) under the hypothesis of local equilibrium adsorption. The equilibrium adsorption model led to best-fitting sigmoids definitely incompatible with the

experimental data (Figs. 4a and 4b, dashed lines), suggesting that mass-transfer phenomena need to be considered in the process simulation.

The second set of simulations (Eqs. (4) and (5)) was conducted under the hypothesis of not negligible mass-transfer resistance and linear isotherm for both PCs and COD. As shown by the best-fitting PC and COD profiles reported in Fig. 4, this approach led for both groups of compounds to satisfactory simulations, with R^2 in the 0.95-0.99 range for PCs and 0.83-0.96 for COD.

The best fitting estimates of $K_{eq,PC}$, $K_{eq,COD}$ and k_{LA} are reported in Table 4. The Gauss-Newton method converged after 6-7 iterations, and provided 95% confidence intervals varying between 2% and 18% of the corresponding best estimates. The low $K_{eq,COD} / K_{eq,PC}$ ratio, equal to 0.11-0.13, confirms the quite high selectivity of the tested resin for PCs. For each studied temperature (21 and 30 °C), the estimates of $K_{eq,PC}$ obtained from the isotherm under the linear approximation (Fig. 2) are significantly lower (28% and 51% decrease, respectively) than the corresponding estimates obtained by best-fit of the breakthrough test. No other works compared the $K_{eq,PC}$ values obtained through an isotherm with those obtained by best-fit of breakthrough tests, to the best of our knowledge. Indeed, few works studied PC adsorption in continuous flow tests [35,36,38], but none of these evaluated $K_{eq,PC}$ by calibrating a transport/adsorption model on the breakthrough data. The deviation between the isotherm and the breakthrough estimates of $K_{eq,PC}$ could be tentatively ascribed to the simplifying approximation of treating all the PCs as a single pseudo-component. Indeed, under this hypothesis all the PCs are assumed to present a single breakthrough curve, whereas the observed experimental trends in the breakthrough tests result from the combination of different, and possibly competing, adsorption curves. This time-changing adsorption equilibrium is not present in the isotherm experiments, where all the PCs are at equilibrium contemporaneously in a static way. As for k_{LA} , the best fit values measured in this work (0.0008 and 0.0025 1/s, at v_{sup} equal to 0.48 and 1.44 m/h respectively) are in agreement with the value reported by Otero et al. [38] (0.0012 1/s, at a v_{sup} equal to 5.7 m/h) for the adsorption of phenol and 4-nitrophenol on a resin analogous to XAD16 (Sephabeads SP206, styrene/divinylbenzene).

The variations of both $K_{eq,PC}$ with temperature and k_{LA} with superficial velocity are in agreement with the theoretical predictions. Indeed, the 9°C temperature increase determined a 20-40% decrease of $K_{eq,PC}$, depending on the estimation method considered (breakthrough test or isotherm). As for k_{LA} , the 3-fold increase in superficial velocity, and therefore in Re number, resulted in a k_{LA} increase proportional to $Re^{1.04}$, whereas the theoretical predictions available for our Re range (0.1-0.2) report a Re exponent equal to 0.33 [60].

The best-fitting PC and COD simulations were used to calculate the PC and COD adsorption yields ($Y_{ads,PC}$ and $Y_{ads,COD}$) and the resin utilization efficiency (η_{resin}) at the selected 20% breakpoint (Table 4). $Y_{ads,PC}$ resulted close to 90%, independently of temperature and superficial velocity. From the same simulated data, the PC adsorption yield and the PC mass fraction in the adsorbed matter (phenolic COD / total COD) were evaluated against dimensionless time (Fig. 4c). The resulting plots show that, as the adsorption time (and therefore the breakthrough concentration) increases, the PC adsorption yield decreases but the selectivity in PCs against COD increases, and a more pure product is thus obtained.

Despite the good selectivity of resin XAD16 for PCs, as a result of the lower content of OMWs in PCs with respect to total COD (the phenolic COD / total COD ratio is typically very

low, 7% for the studied OMW) even at very high dimensionless times the purity of the final product is low ($< 30\%$). Indeed, if a process strategy to maximize $Y_{ads,PC}$ is chosen, only a modest concentration of PCs in the COD of the final product is achieved; on the contrary, if the maximization of PCs in the desorbed product is privileged (with a considerable PC loss in the treated OMW) the selectivity of XAD16 for PCs allows to obtain a 4 fold increase of the PC/COD ratio.

Some work was done to characterize the COD in both the desorbed product and the treated OMW obtained in test bt 2. The analyses showed that carbohydrate concentration in the treated OMW was reduced from 23 to 7 g/L (in good agreement with the 70% adsorption yield calculated from the experimental data model simulation), whereas proteins were completely adsorbed. The residual carbohydrate concentration in the treated OMW did not lead to any observable inhibition effect in the subsequent anaerobic digestion process [46]. With regard to the desorbed product, the analyses showed that the non-phenolic COD was composed by carbohydrates (84%) and proteins (16%).

Notwithstanding the low PC content of the desorbed product, the possible need of a further purification step depends on the specifications requested. Indeed, preliminary evaluations of the antioxidant power of PC/COD mixtures obtained from Imperia OMWs and characterized by a 0.08-0.10 PC mass fraction resulted in a quite high antioxidant capacity (20-25 mM ascorbic acid equivalent). Different purification technologies can be applied to separate most of the non-phenolic COD, so as to obtain a purified, valuable product. Membrane technologies are particularly promising for concentrating and purifying bioactive phenolic compounds from water and for the separation of PCs from macromolecules such as proteins; moreover, membranes can be used to separate high molecular weight PCs, such as verbascoside, from low molecular weight ones such as hydroxytyrosol [61-64]. Alternatively, single PCs can be retained by means of molecular fingerprinting adsorption processes, based on the use of polymers characterized by the presence of active sorption sites with a high selectivity for specific high-value PCs, such as tyrosol and hydroxytyrosol [13,65,66].

3.5 *Desorption-regeneration tests*

The adsorbed matter (PCs and other COD) was desorbed from the resin and the column was regenerated by feeding acidified ethanol (0.5% v/v HCl 0.1N) according to the procedure described in Section 2.8. The dimensionless desorption curves are not shown because the ethanol flow rate was adjusted manually in order to maintain the total pressure at the column inlet < 2 bars. The PC desorption yield varied between 65% and 74% (Table 4). In an earlier batch work conducted by the same research group with XAD16 [28] a lower desorption yield was obtained (53%), whereas other authors obtained complete desorption of PCs from different adsorbents using different ethanol/water mixtures [37,59]. Agalias et al. [35] worked with an actual OMW and with the XAD 16 resin, and reported a successful PC desorption using an ethanol/isopropanol mixture. These works showed that an almost quantitative recovery of PCs from XAD16 is possible and that an optimization of the desorption step in the continuous-flow process is needed.

3.6 *Pilot-plant model-based preliminary design*

In order to identify the optimal column length for a potential scale-up of the process, the 1-D model of dispersion, convection and non-equilibrium adsorption and the best fitting estimates of $K_{eq,Ph}$, $K_{eq,COD}$ and k_{LA} obtained at 1.44 m/h and 30°C (Table 4, 3rd column) were used to simulate the behavior of adsorption columns characterized by different lengths in the 0.5-10 m range. As shown in Fig. 5, both the PC adsorption yield and the resin utilization efficiency – evaluated at a 20% breakthrough point – increase with bed length. Although a complete economic optimization of the process is beyond the scope of this work, a preliminary analysis indicates that as $Y_{ads,PC}$ – and therefore the column length – increases, the gains associated to PC selling increase, but also the operational cost related to pressure drop and the column capital cost increase. Furthermore, an increase in column length leads to a higher resin utilization efficiency, and therefore to a lower yearly cost associated to the periodic resin replacement. Indeed, the duration of each adsorption step (or breakthrough time, t_{bt}) can be evaluated as:

$$t_{bt} = \frac{m_{PC,sorbed,bt}/Y_{ads,PC}}{\dot{m}_{PC,IN}} = \frac{m_{PC,sorbed,sat} \cdot \eta_{resin}}{\dot{m}_{PC,IN} \cdot Y_{ads,PC}} = \frac{K_{eq,PC} \cdot \rho_b \cdot S_t \cdot L \cdot C_{PC,IN} \cdot \eta_{resin}}{Q \cdot C_{PC,IN} \cdot Y_{ads,PC}} \quad (11)$$

Thus, assuming that 2 columns work in parallel with adsorption and desorption cycles of equal length, the resin operational time t_{resin} can be expressed as:

$$t_{resin} = 2 \cdot t_{bt} \cdot n_{cycles} = 2 \cdot n_{cycles} \cdot \frac{K_{eq,PC} \cdot \rho_b \cdot S_t \cdot L \cdot \eta_{resin}}{Q \cdot Y_{ads,PC}} \quad (12)$$

where n_{cycles} – the number of adsorption and desorption cycles that can be performed with one resin load – is a crucial parameter to be evaluated for each resin. Eq. (12) is based on the assumption that n_{cycles} does not depend on η_{resin} . Ultimately, the yearly cost for the periodic resin replacement is given by:

$$C_{resin} = \frac{m_{resin} \cdot SC_{resin}}{t_{resin}} = \frac{2 \cdot \rho_b \cdot S_t \cdot L \cdot SC_{resin}}{t_{resin}} = \frac{Q \cdot SC_{resin} \cdot Y_{ads,PC}}{n_{cycles} \cdot K_{eq,PC} \cdot \eta_{resin}} \quad (13)$$

Therefore, the yearly resin cost is inversely proportional to the resin efficiency.

Although the exact identification of the optimal column length requires a quantitative evaluation of these aspects, the observation of Fig. 5 indicates that at lengths in the 2-4 m range the increase in adsorption yield is almost complete and the bed efficiency increases with a much lower slope. Thus, a column length of 2-4 m can be preliminary identified as the right one to further develop and optimize the process.

4 Conclusions

The continuous-flow PC adsorption, desorption and recovery process proved to be feasible, reliable and effective. Despite the high selectivity of the XAD16 resin for PCs, the PC purity in the finale product resulted < 30% as a result of the very low (phenolic COD / total COD) ratio of the tested OMW. The experimental work, conducted with a relatively shallow adsorption bed (0.53 m), led to the development of a reliable model of the process, based on the assumption of non-equilibrium adsorption and characterized by an overall mass transfer resistance. The model parameters were estimated with a high accuracy and fitting quality. The model was utilized to estimate the process performances and to perform a preliminary evaluation of the optimal column length for a pilot plant, to be utilized for a further process optimization and a more robust assessment of the process performances. As a secondary outcome of this work, an effective OMW pre-treatment was developed and an analytical HPLC method more precise and less time-consuming than the traditional FC method was set up and validated. Overall, this study represents an important step towards the development, modeling and preliminary optimization of a continuous

flow adsorption/desorption process aimed at OMW PC separation. Further research is needed to optimize the desorption step, to evaluate the number of adsorption/desorption cycles that can be performed with the same resin, and to perform an overall economic optimization of the process.

Acknowledgements

Project co-funding by the European Commission under Grant Agreement n. 311933 (Water4Crops project, 7th FP) is acknowledged. The authors wish to thank Dino Ibba for his contribution to the experimental work.

List of symbols

A_s	Asymmetry factor (-)
$C_{L,i}$	Liquid phase concentration of compound i (mg/L)
$\bar{C}_{L,measured}$	Average liquid phase concentration measured during a given experiment (mg/L)
$C_{L,PC,0}$ $C_{L,PC,eq}$	Initial and final (equilibrium) PC concentration in the liquid phase (OMW) during the isotherm tests (mg _{PC} /L)
C_{resin}	Yearly cost for the periodic resin replacement (€/y)
$C_{S,i}$	Solid phase (resin) concentration of compound i (mg/ g _{dry resin})
$C_{S,PC,eq}$	Final (equilibrium) PC concentration in the solid phase (resin) during the isotherm tests (mg _{PC} /g _{dry resin})
D_{eq}	Equivalent diffusion coefficient, calculated as $\alpha_L \cdot v_{int}$
d_p	Average size of the packing particles (m)
$HETP$	Height equivalent to a theoretical plate, in the packed column (m)
HRT	Hydraulic residence time in the column, calculated as $V_{resin} \cdot \epsilon_{resin} / Q + V_{sand} \cdot \epsilon_{sand} / Q$ (s)
$K_{eq,i}$	Adsorption constant of compound i , defined as the slope of the linear portion of the isotherm (L _{pore volume} / kg _{dry resin}). A further subscript, if present, indicates the temperature.
$k_L a$	Mass transfer coefficient (1/s)
L	Column length (m)
$\dot{m}_{PC,IN}$	PC mass flow rate entering the column (mg/s)
$m_{PC,sorbed,bt}$	PC mass adsorbed by the resin at time t_{bt} (mg)
$m_{PC,sorbed,sat}$	PC mass theoretically adsorbed by the resin upon saturation of the sorption capacity (mg)
m_S	Mass of dry resin in the isotherm studies (g _{dry resin})

N	Number of experimental data used to calculate each R^2 value (-)
n_{cycles}	Number of adsorption and desorption cycles that can be performed with one resin load (-)
N_{tp}	Number of theoretical plates in the column packing (-)
P	Number of parameters estimated in each model calibration (-)
Q	Volumetric flow rate through the column (m^3/s)
SC_{resin}	Resin specific cost (€/kg)
S_t	Column section (m^2)
t_{bt}	Breakthrough time (s)
t_R	Retention time of the RTD curve, in the fluid-dynamic tests (s)
t_{resin}	Resin operational time (s)
v_{sup}	Superficial velocity (m/s)
v_{int}	Interstitial velocity (m/s)
$w_{1/2}$	Width of the RTD curve at half-height, in the fluid-dynamic tests (s)
$Y_{ads,i}$	Adsorption yield of compound i in a breakthrough test, calculated as $m_{i,sorbed,20\%} / m_{i,fed,20\%}$ (-)
α_L	Longitudinal dispersivity (m)
δ_i	Retardation factor δ_i , calculated as $1 + K_{eq,i} \rho_b / \varepsilon$ (-)
ε	Effective porosity (-)
η_{resin}	Resin utilization efficiency, calculated as $m_{PC,sorbed,20\%} / m_{PC,sorbed,sat}$ (-)
ρ_b	Resin bulk density (kg / m^3)

References

- [1] L. Tuck, P.J. Hayball, Major phenolic compounds in olive oil: metabolism and health effects, J. Nutr. Biochem. 13 (2002) 636-644.
- [2] S. Dermeche, M. Nadour, C. Larroche, F. Moulti-Mati, P. Michaud, Olive mill wastes: biochemical characterizations and valorization strategies, Process Biochem. 48 (2013) 1532–1552.
- [3] P.S. Rodis, V. T. Karathanos, A. Mantzavinou, Partitioning of olive oil antioxidants between oil and water phases, J. Agric. Food Chem. 50 (2002) 596–601.

- [4] International Olive Council, 2015. <http://www.internationaloliveoil.org/estaticos/view/131-world-olive-oil-figures> (accessed on May 10, 2015).
- [5] L.C. Davies, A.M. Vilhena, J.M. Novais, S. Martins-Dias, Olive mill wastewater characteristics: modelling and statistical analysis, *Grasas Aceites* 55 (2004) 233-241.
- [6] L. Bertin, F. Ferri, A. Scoma, L. Marchetti, F. Fava, Recovery of high added value natural polyphenols from actual olive mill wastewater through solid phase extraction, *Chem. Eng. J.* 171 (2011) 1287– 1293.
- [7] T. Yangui, S. Sayadi, A. Gargoubi, A. Dhouib, Fungicidal effect of hydroxytyrosol-rich preparations from olive mill wastewater against *Verticillium dahlia*, *Crop Protection* 29 (2010) 1208-1213.
- [8] N. Rahmanian, S.M. Jafari, C.M. Galanakis, Recovery and removal of phenolic compounds from olive mill wastewater, *J. Am. Oil Chem. Soc.* 91 (2014) 1–18.
- [9] G. Pekin, S. Haskök, S. Sargin, Y. Gezgin, R. Eltem, E. İkizoğlu, N. Azbar, F.V. Sukan, Anaerobic digestion of Aegean olive mill effluents with and without pretreatment, *J. Chem. Technol. Biotechnol.* 85 (2010) 976-982.
- [10] A. El-Abbassi, H. Kiai, A. Hafidi, Phenolic profile and antioxidant activities of olive mill wastewater, *Food Chem.* 132 (2012) 406-412.
- [11] N. Kalogerakis, M. Politi, S. Foteinis, E. Chatzisyneon, D. Mantzavinos, Recovery of antioxidants from olive mill wastewaters: a viable solution that promotes their overall sustainable management, *J. Environ. Manage.* 128 (2013) 749-758.
- [12] C. Fortes, J.A. García-Vilas, A.R. Quesada, M.A. Medina, Evaluation of the anti-angiogenic potential of hydroxytyrosol and tyrosol, two bio-active phenolic compounds of extra virgin olive oil, in endothelial cell cultures, *Food Chem.* 134 (2012) 134-140.
- [13] F. Puoci, A. Scoma, G. Cirillo, L. Bertin, F. Fava, N. Picci, Selective extraction and purification of gallic acid from actual site olive mill wastewaters by means of molecularly imprinted microparticles, *Chem. Eng. J.* 198-199 (2012) 529–535.
- [14] T.A. Lafka, A.E. Lazou, V.J. Sinanoglou, E.S. Lazos, Phenolic and antioxidant potential of olive oil mill wastes, *Food Chem.* 125 (2011) 92–98.
- [15] A. De Leonardis, V. Macciola, G. Lembo, A. Aretini, A. Nag, Studies on oxidative stabilization of lard by natural antioxidants recovered from olive oil mill wastewater, *Food Chem.* 100 (2007) 998-1004.
- [16] C.M. Galanakis, E. Tornberg, V. Gekas, Recovery and preservation of phenols from olive waste in ethanolic extracts, *J. Chem. Technol. Biotechnol.* 85 (2010) 1148-1155.
- [17] T.J. Klen, B.M. Vodopivec, Ultrasonic extraction of phenols from olive mill wastewater: comparison with conventional methods, *J. Agr. Food Chem.* 59 (2011) 12725-12731.
- [18] A. El-Abbassi, H. Kiai, J. Raiti, A. Hafidi, Application of ultrafiltration for olive processing wastewaters treatment, *J. Cleaner Prod.* 65 (2014) 432-438.

- [19] D.P. Zagklisa, A.I. Vavourakia, M.E. Kornarosa, C.A. Paraskevaa, Purification of olive mill wastewater phenols through membrane filtration and resin adsorption/desorption, *J. Hazard. Mater.* 285 (2015) 69–76.
- [20] E. Garcia-Castello, A. Cassano, A. Criscuoli, C. Conidi, E. Drioli, Recovery and concentration of polyphenols from olive mill wastewaters by integrated membrane system, *Water Res.* 44 (2010) 3883–3892.
- [21] C. Conidi, R. Mazzei, A. Cassano, L. Giorno, Integrated membrane system for the production of phytotherapies from olive mill wastewaters, *J. Membr. Sci.* 454 (2014) 322–329.
- [22] A. El-Abbassi, H. Kiai, J. Raiti, A. Hafidi, Cloud point extraction of phenolic compounds from pretreated olive mill wastewater, *J. Environ. Chem. Eng.* 2 (2014) 1480–1486.
- [23] O. Gortzi, S. Lalas, A. Chatzilazarou, E. Katsoyannos, S. Papaconstandinou, E. Dourtoglou, Recovery of natural antioxidants from olive mill wastewater using Genapol-X080, *J. Am. Oil Chem. Soc.* 85 (2008) 133–140.
- [24] C.M. Galanakis, Emerging technologies for the production of nutraceuticals from agricultural by-products: a viewpoint of opportunities and challenges, *Food Bioprod. Processing* 91 (2013) 575–579.
- [25] C.M. Galanakis, A. Schieber, Editorial, *Food Res. Int.* 65 (2014) 299–300.
- [26] M.L. Soto, A. Moure, H. Domínguez, J.C. Parajó, Recovery, concentration and purification of phenolic compounds by adsorption: a review, *J. Food Eng.* 105 (2011) 1–27.
- [27] F. Ferri, L. Bertin, A. Scoma, L. Marchetti, F. Fava, Recovery of low molecular weight phenols through solid-phase extraction, *Chem. Eng. J.* 166 (2011) 994–1001.
- [28] A. Scoma, C. Pintucci, L. Bertin, P. Carlozzi, F. Fava, Increasing the large scale feasibility of a solid phase extraction procedure for the recovery of natural antioxidants from olive mill wastewaters, *Chem. Eng. J.* 198–199 (2012) 103–109.
- [29] M.A. Abdullah, L. Chiang, M. Nadeem, Comparative evaluation of adsorption kinetics and isotherms of a natural product removal by Amberlite polymeric adsorbents, *Chem. Eng. J.* 146 (2009) 370–376.
- [30] A.K. Sandhu, L. Gu, Adsorption/desorption characteristics and separation of anthocyanins from muscadine (*Vitis rotundifolia*) juice pomace by use of macroporous adsorbent resins, *J. Agric. Food Chem.* 61 (2013) 1441–1448.
- [31] F.A. Tomás-Barberán, M.A. Blázquez, A comparative study of different Amberlite XAD resins in flavonoid analysis, *Phytochem. Analysis* 3 (1992) 178–181.
- [32] E.M. Silva, D.R. Pompeu, Y. Larondelle, H. Rogez, Optimisation of the adsorption of polyphenols from *Inga edulis* leaves on macroporous resins using an experimental design methodology, *Sep. Purif. Technol.* 53 (2007) 274–280.
- [33] M.L. Soto, E. Conde, N. González-López, M.J. Conde, A. Moure, J. Sineiro, E. Falqué, H. Domínguez, M.J. Núñez, J.C. Parajó, Recovery and concentration of antioxidants from winery wastes, *Molecules* 17 (2012) 3008–3024.

- [34] M. Monsanto, R. Mestrom, E. Zondervan, P. Bongers, J. Meuldijk, Solvent swing adsorption for the recovery of polyphenols from black tea, *Ind. Eng. Chem. Res.* 54 (2015) 434–442.
- [35] A. Agalias, P. Magiatis, A-L. Skaltsounis, E. Mikros, A. Tsarbopoulos, E. Gikas, I. Spanos, T. Manios, A new process for the management of olive oil mill waste water and recovery of natural antioxidants, *J. Agric. Food Chem.* 55 (2007) 2671-2676.
- [36] D. R. Kammerer, R. Carle, R.A. Stanley, Z.S. Saleh, Pilot-scale resin adsorption as a means to recover and fractionate apple polyphenols, *J. Agric. Food Chem.* 58 (2010) 6787–6796.
- [37] T.J. Buran, A.K. Sandhu, Z. Li, C.R. Rock, W.W. Yang, L. Gu, Adsorption/desorption characteristics and separation of anthocyanins and polyphenols from blueberries using macroporous adsorbent resins, *J. Food Eng.* 128 (2014) 167–173.
- [38] M. Otero, M. Zabkova, A.E. Rodrigues, Phenolic wastewaters purification by thermal parametric pumping: modeling and pilot-scale experiments, *Water Res.* 39 (2005) 3467–3478.
- [39] J. Kim, M. Yoon, H. Yang, J. Jo, D. Han, Y.J. Jeon, S. Cho, Enrichment and purification of marine polyphenol phlorotannins using macroporous adsorption resins, *Food Chem.* 162 (2014) 135–142.
- [40] K. Chen, H. Lyu, S. Hao, G. Luo, S. Zhang, J. Chen, Separation of phenolic compounds with modified adsorption resin from aqueous phase products of hydrothermal liquefaction of rice straw, *Biores. Technol.* 182 (2015) 160–168.
- [41] Y. Liu, Q. Bai, Y. Liu, D. Di, M. Guo, L. Zhao, J. Li, Simultaneous purification of tea polyphenols and caffeine from discarded green tea by macroporous adsorption resins, *Eur. Food Res. Technol.* (2014) 238:59–69.
- [42] J. Huang, L. Yang, X. Wub, M. Xu, Y.N. Liu, S. Deng, Phenol adsorption on α,α' -dichloro-p-xylene (DCX) and 4,4'-bis(chloromethyl)-1,1'-biphenyl (BCMBP) modified XAD-4 resins from aqueous solutions, *Chem. Eng. J.* 222 (2013) 1–8.
- [43] B.C. Pan, F.W. Meng, X.Q. Chen, B.J. Pan, X.T. Li, W.M. Zhang, X. Zhang, J.L. Chen, Q.X. Zhang, Y. Sun, Application of an effective method in predicting breakthrough curves of fixed-bed adsorption onto resin adsorbent, *J. Hazard. Mater.* B124 (2005) 74–80.
- [44] S.H. Lin, C.H. Wang, H.G. Leu, A theoretical model for predicting column phenol adsorption by macroporous resin, *J. Environ. Sci. Heal. A* 34 (1999) 1283-1297.
- [45] C.M. Galanakis, Recovery of high added-value components from food wastes: conventional, emerging technologies and commercialized applications, *Trends Food Sci. Tech.* 26 (2012) 68-87.
- [46] G.A. Martinez, L. Bertin, A. Scoma, S. Rebecchi, G. Braunegg, F. Fava, Production of polyhydroxyalkanoates from dephenolised and fermented olive mill wastewaters by employing a pure culture of *Cupriavidus necator*. *Biochem. Eng. J.* 97 (2015) 92-100.
- [47] O. Folin, V. Ciocalteu, On tyrosine and tryptofan determinations in protein, *J. Biol. Chem.* 73 (1927) 627–650.

- [48] M.F. Chaplin, Monosaccharides. In: Chaplin MF, Kennedy JF, editors. Carbohydrate analysis-a practical approach. 2nd ed, New York: Oxford University Press, Inc; 1994. 1–41.
- [49] C.S. Frings, T.W. Fendley, R.T. Dunn, C.A. Queen, Improved determination of total serum lipids by the sulfo-phospho-vanillin reaction, *Clinical Chem.* 18 (1972) 673–674.
- [50] M.M. Bradford, A rapid and sensitive method for the quantitation of microgram quantities of protein utilizing the principle of protein-dye binding, *Anal. Biochem.* 72 (1976) 248–254.
- [51] O. Levenspiel, *Chemical Reaction Engineering*, third ed., Wiley, New York, 1999.
- [52] GE Healthcare Bio-Sciences AB, Column efficiency testing - Application note 28-9372-07 AA, Uppsala, Sweden, 2010. https://www.gelifesciences.com/gehcls_images/GELS/Related%20Content/Files/1352880951136/litdoc28937207_20141127221416.pdf (accessed on May 20, 2015).
- [53] C.W. Fetter, *Applied Hydrogeology*, fourth ed., Prentice Hall, Upper Saddle River, New Jersey, 2001.
- [54] P. Englezos, N. Kalogerakis, *Applied parameter estimation for chemical engineers*, Marcel Dekker, New York – Basel, 2001.
- [55] F. Zama, R. Ciavarelli, D. Frascari, D. Pinelli, Numerical parameter estimation in models of pollutant transport with chemical reaction, in: *IFIP Advances in Information and Communication Technology*, vol. 391, D. Homberg, F. Troltsch (Eds.), System Modeling and Optimization, Springer, Heidelberg, 2013, pp. 547 – 556.
- [56] A.S. Rathore, R.M. Kennedy, J.K. O'Donnell, I. Bemberis, O. Kaltenbrunner, Qualification of a chromatographic column. Why and how to do it, *BioPharm International* 16 (2003) 30–40.
- [57] W.L. McCabe, J.C. Smith, P. Harriott, *Unit Operations of Chemical Engineering*, sixth ed., McGraw-Hill, New Ork, 2001.
- [58] D. Frascari, S. Fraraccio, M. Nocentinia, D. Pinelli, Trichloroethylene aerobic cometabolism by suspended and immobilized butane-growing microbial consortia: a kinetic study. *Biores. Technol.* 1244 (2013) 529–538.
- [59] X. Wang, P.D. Patil, C. He, J. Huang, Y.N. Liu, Acetamide-modified hyper-cross-linked resin: synthesis, characterization, and adsorption performance to phenol from aqueous solution. *J. Appl. Polym. Sci.* 132 (2015) 4197.
- [60] R. Perry, D. Green, *Perry's Chemical Engineers' Handbook*, eighth ed., McGraw-Hill, New York, 2008.
- [61] C.M. Galanakis, Separation of functional macromolecules and micromolecules: from ultrafiltration to the border of nanofiltration, *Trends Food Sci. Tech.* 42 (2015) 44–63.
- [62] C.M. Galanakis, E. Tornberg, V. Gekas, Clarification of high-added value products from olive mill wastewater, *J. Food Eng.* 99 (2010) 190–197.

- [63] I. D'Antuono, V.G. Kontogianni, K. Kotsiou, V. Linsalata, A.F. Logrieco, M.Tasioula-Margari, A. Cardinali, Polyphenolic characterization of olive mill wastewaters, coming from Italian and Greek olive cultivars, after membrane technology, *Food Res. Int.* 65 (2014) 301–310.
- [64] C. Russo, A new membrane process for the selective fractionation and total recovery of polyphenols, water and organic substances from vegetation waters (VW), *J. Membr. Sci.* 288 (2007) 239–246.
- [65] P. Xiao, P. F.-X. Corvini, Y. Dudal, P. Shahgaldian, Design and high-throughput synthesis of cyclodextrin-based polyurethanes with enhanced molecular recognition properties, *Polym. Chem.* 4 (2013) 942-946.
- [66] P. Xiao, P. F.-X. Corvini, Y. Dudal, P. Shahgaldian, Design of cyclodextrin-based photopolymers with enhanced molecular recognition properties: a template-free high-throughput approach, *Macromolecules* 45 (2012) 5692-5697.

Table 1

Main characteristics of the tested “Imperia 2012” OMW.

Total PCs (g/L)	2.0
Total solids (g/L)	34.0
Suspended solids (g/L)	0.7
Dissolved solids (g/L)	33.3
COD (g/L)	31.5
Total Carbohydrates (g/L)	23
Total Lipids (g/L)	< 0.1
Total Proteins (g/L)	3
Density (kg/L)	1.01
pH	4.60

Table 2

Technical characteristics of adsorption resin Amberlite XAD 16.

Matrix	Macroreticular aliphatic crosslinked polymer (styrene / divinylbenzene)
Physical form	White translucent beads
Specific density (kg/L)	1.039
Adsorption capacity at saturation (mg/g _{dry resin}) ^a	370
Surface area (m ² /g)	800
Porosity (dry resin; L/L)	0.55
Average particle size (dry resin; mm)	0.63
Uniformity coefficient	2.0
Fines content (mm)	< 0.350: 2.0% max
Coarse content (mm)	> 1.18: 2.0% max
Maximum reversible swelling	25% (on p-xylene via methanol)

^a Referred to medium molecular weight compounds

Table 3

PC concentrations measured in two distinct OMWs with the Folin Ciocalteu colorimetric method and with the HPLC method: average values \pm 95% confidence intervals.

OMW type	Imperia 2012	Gallipoli 2012
Folin-Ciocalteu method (g/L)	1.96 ± 0.37	4.14 ± 0.81
HPLC method (g/L)	1.26 ± 0.09	2.79 ± 0.16
Deviation between the two methods	36%	33%

Table 4

Fluid-dynamic, adsorption and desorption performances relative to the two breakthrough tests and to the two isotherms.

Parameter	Bt 1 (21°C, 0.48 m/h)	Bt 2 (30°C, 1.44 m/h)
Bulk density (ρ_b , kg _{dry resin} /L)	0.908	0.870
Resin longitudinal dispersivity ($\alpha_{L,resin}$, m)	$(4.1 \pm 0.2) \cdot 10^{-3}$	$(4.0 \pm 0.2) \cdot 10^{-3}$
Resin porosity (ε_{resin} , -)	0.85	0.83
PC adsorption yield ($Y_{ads,PC}$, -) ^a	87.1%	87.9%
COD adsorption yield ($Y_{ads,COD}$, -) ^a	60.7%	74.8%
Resin utilization efficiency (η_{resin} , -) ^a	16.8%	12.2%
PC desorption yield ($Y_{des,PC}$, -)	65.1%	74.0%
k_{La} (1/s)	$(0.8 \pm 0.1) \cdot 10^{-3}$	$(2.5 \pm 0.2) \cdot 10^{-3}$
$K_{eq,COD}$ (L _{pore volume} / kg _{dry resin}) ^b	11 ± 1	11 ± 2
$K_{eq,PC}$ (L _{pore volume} / kg _{dry resin}) ^b	102 ± 16	85 ± 2
$K_{eq,PC}$ (L _{pore volume} / kg _{dry resin}) ^c	73 ± 12	42 ± 6

^a Evaluated at a 20% PC outlet normalized concentration.

^b Evaluated by best-fit of the breakthrough tests with the 1-D convection/dispersion model with mass-transfer.

^c Evaluated from the isotherms.

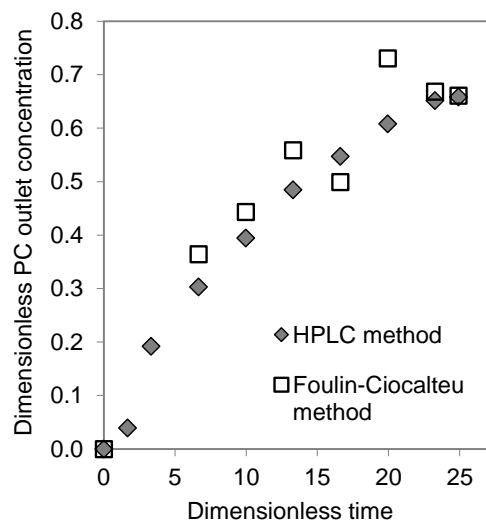


Fig. 1. Dimensionless outlet PC concentration versus dimensionless time for breakthrough test bt 2 (30°C, $v_{sup} = 1.44$ m/h): comparison between the HPLC method and the Foulin-Ciocalteu method.

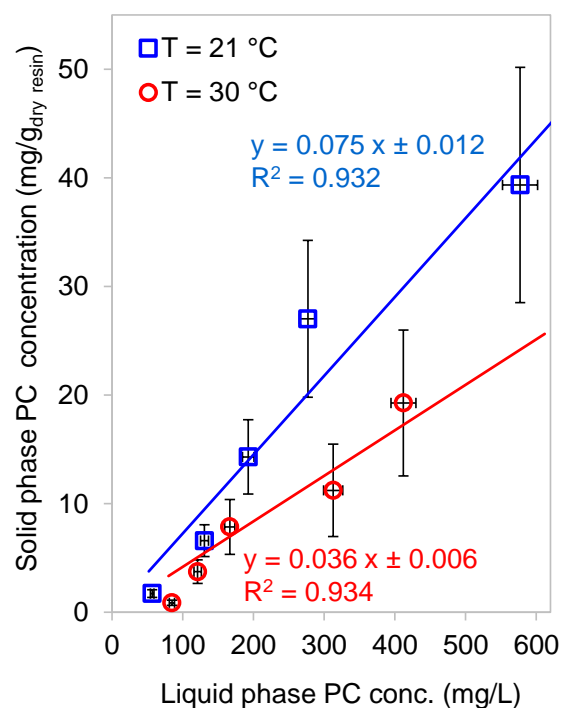


Fig. 2. Solid- and liquid-phase PC concentrations relative to the isotherms performed at 21°C and 30°C, with best-fitting linear interpolations.

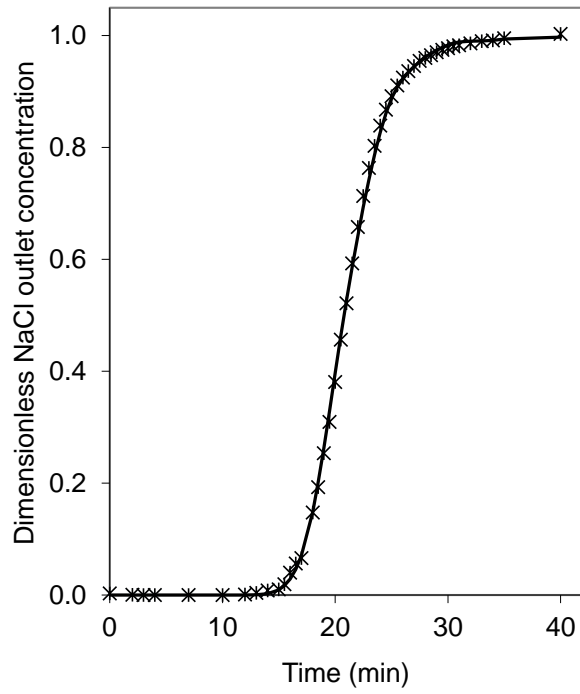


Fig. 3. Fluid-dynamic test performed before breakthrough test bt 1: experimental dimensionless NaCl concentration at the column exit and corresponding best-fitting simulation performed with Eq. (3).

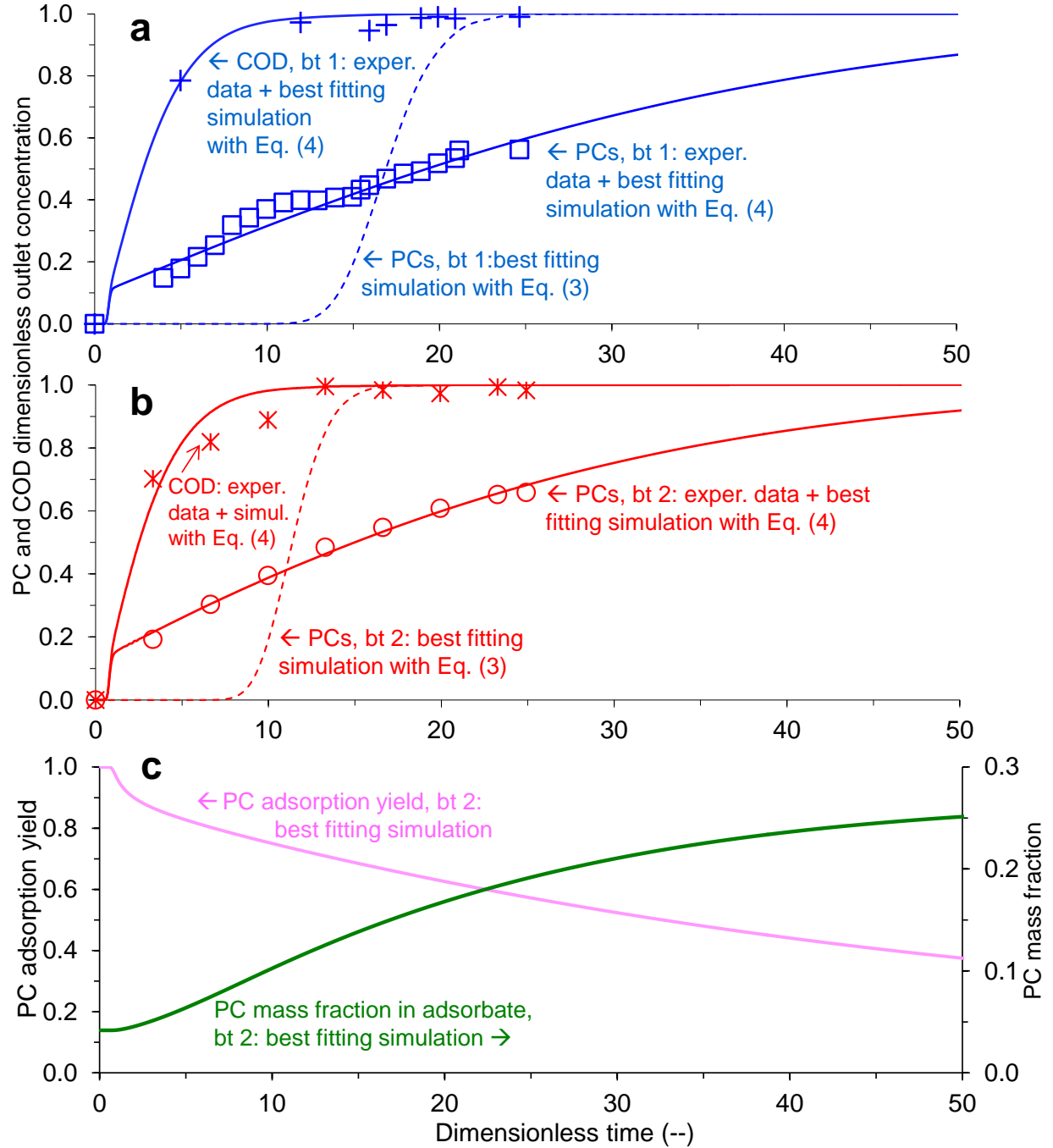


Fig. 4. (a) Experimental and simulated outlet normalized COD and PC concentrations relative to adsorption test bt 1 (21°C, $v_{sup} = 0.48$ m/h); (b) experimental and simulated outlet normalized COD and PC concentrations relative to adsorption test bt 2 (30°C, $v_{sup} = 1.44$ m/h); (c) model-based evaluation of the PC adsorption yield and PC mass fraction in the adsorbate relative to test bt 2 (30°C, $v_{sup} = 1.44$ m/h). The simulations based on the 1-D model with equilibrium adsorption (Eq. (3)) are reported with dashed lines, whereas those based on the 1-D model with non-equilibrium adsorption (Eqs. (4) and (5)) are reported with continuous lines.

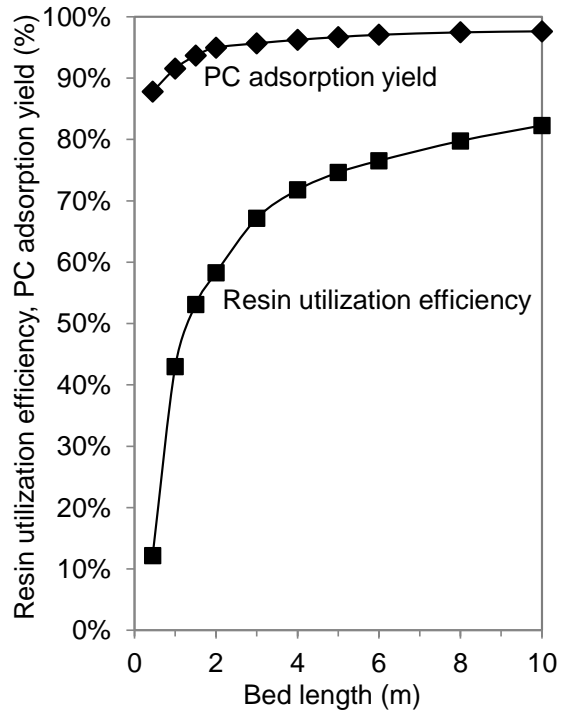


Fig. 5. PC adsorption yield and resin utilization efficiency at a 20% breakthrough point evaluated for columns of different lengths, using the best-fitting parameters estimated at $T = 30^{\circ}\text{C}$ and $v_{sup} = 1.44 \text{ m/h}$.